

The angular power spectra of polarized Galactic synchrotron

M. Tucci^{a,b,1}, E. Carretti^{c,2}, S. Cecchini^{c,3}, R. Fabbri^{d,4},
M. Orsini^{c,e,5}, E. Pierpaoli^{f,6}

^a*Dipartimento di Fisica G. Occhialini, Università di Milano, Bicocca
I.N.F.N., Sezione di Milano, Via Celoria 16, I-20133 Milano, Italy*

^b*I.Te.S.R.E.-C.N.R., Via P. Gobetti 101, I-40129 Bologna, Italy*

^d*Dipartimento di Fisica, Università di Firenze, Via S. Marta 3, I-50139 Firenze,
Italy*

^e*Dipartimento di Astronomia, Università di Bologna, Via Ranzani 1, I-40127
Bologna, Italy*

^f*Department of Physics and Astronomy, University of British Columbia, 2219
Main Mall, Vancouver, B.C. V6T 1Z4, Canada*

Abstract

We derive the angular power spectra of intensity and polarization of Galactic synchrotron emission in the range $36 \leq \ell \lesssim 10^3$ from the Parkes survey mapping the southern Galactic plane at 2.4 GHz. The polarization spectra of both electric and magnetic parity up to $\ell \simeq 10^3$ are approximated very well by power laws with slope coefficients $\simeq 1.4$, quite different from the CMB spectra. We show that no problem should arise from Galactic synchrotron for measurements of CMB polarization in the cosmological window.

Key words: Background radiations — Radio continuum: general — Methods: statistical

PACS: 98.70-f, 98.70.Vc

¹ E-mail: marco@axrialto.uni.mi.astro.it

² E-mail: carretti@tesre.bo.cnr.it

³ E-mail: cecchini@bo.infn.it

⁴ E-mail: fabbri@dfs.unifi.it;fabbri@ff.infn.it

⁵ E-mail: orsini@tesre.bo.cnr.it

⁶ E-mail: elena@astro.ubc.ca

1 Introduction and main results

The purpose of this work is to compute the angular power spectra of synchrotron emission from the Galaxy, and in particular of its polarized component. Synchrotron radiation is expected to dominate the linearly polarized component of the sky background in a wide frequency range up to a few tens of GHz. It is important for the knowledge of the Galactic structure, and also because it will be a major contaminant in forthcoming measurements of the polarization of the cosmic microwave background (CMB), planned from ground (Keating et al., 1998; Sironi et al., 1997; Pisano, 1999; Hedman, 1999) and from space (Wright, 1999; Cortiglioni et al., 1999; De Zotti et al., 1999).

Separation of the various contributions to the total background in the “cosmological window” (say, $\simeq 50 - 90$ GHz) promises to be a delicate job, and its success will rely on sensible assumptions about the spectral and spatial properties of Galactic foregrounds (e.g., Tegmark et al. 2000, Prunet et al. 2000). In this connection we observe that at frequencies of tens of GHz the dominant contribution to the angular spectrum may be a Galactic foreground (synchrotron or dust), the integrated background of unresolved extragalactic sources, the primordial anisotropy of CMB or a non-primordial anisotropy (for instance arising from the gravitational lens effect) depending on the range of the spherical-harmonic index l . Therefore the cosmological window should be understood as a bidimensional region of the (ν, l) plane, which is furthermore different for anisotropy and polarization. For this reason angular power spectra, which provide a standard tool for CMB analysis, are becoming relatively commonplace also for foregrounds, although in the latter case they provide an incomplete description because of the strong phase coherence of Galactic emission. Intensity (or temperature) power spectra of foregrounds are reasonably approximated by power laws, $C_{l\ell} \propto \ell^{-\alpha_l}$, with slopes steeper than CMB. For the latter the scale-invariant adiabatic-wave spectrum predicts $\alpha_l^{\text{CMB}} \simeq 2$ on large scales and power excess at $10^2 \lesssim \ell \lesssim 10^3$ because of several acoustic peaks. Both the large-scale behaviour and the first acoustic peak appear to be confirmed by experiment (Barreiro, 1999, de Bernardis et al. 2000, Hanany et al. 2000). For synchrotron, values $\alpha_l^{\text{syn}} \simeq 2.5 \div 3$ have been derived from the 408-MHz maps of Haslam et al. (1981) by Tegmark & Efstathiou (1996) and Bouchet et al. (1996), and $\alpha_l^{\text{syn}} \simeq 3$ from the 1420-MHz northern sky survey (Reich & Reich, 1986) by Bouchet & Gispert (1999). However, the analysis of Tenerife patch at the same frequencies provides a nearly scale-invariant spectrum, $\alpha_l^{\text{syn}} \simeq 2$, except near the resolution limit of the maps (Lasenby, 1997). For dust emission Gautier et al. (1992) gave $\alpha_l^{\text{dust}} \simeq 3$ down to the IRAS resolution of a few arc minutes, and a similar result was found for DIRBE (Wright, 1998); from the combined DIRBE and IRAS maps Schlegel et al. (1998) derive $\alpha_l^{\text{dust}} \simeq 2.5$. The situation is less clear for free-free emission: While Kogut et al. (1996) find $\alpha_l^{\text{FF}} \simeq 3$ correlating COBE-DMR with DIRBE,

Veeraraghavan & Davies (1997) derive $\alpha_I^{\text{FF}} \simeq 2.3$ at 53 GHz from H α maps but with a *much lower* normalization. The discrepancy supports the case for dust emission in the cosmological window, the mechanism of rotational excitation of small grains having been proposed by Draine & Lazarian (1998).

Angular spectra of polarized emission have been measured so far neither for CMB nor for Galactic foregrounds. Theoretical modeling for CMB gives (for the electric-parity polarization excited by density waves in the standard-model) α_E^{CMB} rather close to zero, which means much smaller spatial correlations at large angular scales than for temperature fluctuations. A corresponding excess of small-scale structure (in comparison to temperature fluctuations) is found by Prunet et al. (1998) for polarized dust emission in modeling based on the HI maps of the Leiden-Dwinglo survey [see also Sethi et al. (1998) and Prunet & Lazarian (1999)]: Their results are $\alpha_E^{\text{dust}} \simeq 1.3$ and $\alpha_B^{\text{dust}} \simeq 1.4$ for the electric and magnetic parity spectra, respectively. The angular power spectrum is therefore steeper for Galactic dust than for CMB.

Now an important question should be posed: can this result be generalized to other foregrounds? If so, the separation of CMB polarization signals would be easier. The present work considers the polarization spectra of Galactic synchrotron, and can be regarded as complementary to that of Prunet et al. (1998) since polarized free-free emission should not be dominant at any frequency. Our approach is the analysis of low-frequency maps. Unfortunately no full-sky survey is available for the polarized component of synchrotron, the largest coverage being provided by Brouw & Spoelstra (1976) at the expense of a quite sparse sampling. Here we make use of the Parkes survey of the southern Galactic plane (Duncan et al., 1995, 1997) which, although limited to a relatively small window of $\simeq 0.39$ sr, provides uniformly covered maps, not suffering from undersampling. Its frequency of 2.4 GHz probably allows a reasonable extrapolation to the cosmological window, thanks to the limited effects expected from Faraday rotation. The typical values of 5–10 rad m⁻² for the rotation measure (RM) reported by Spoelstra (1984) and Wieringa et al (1993) allow to estimate a negligible depolarization of few percent at 2.4 GHz.

The main result of this paper is that the synchrotron polarization spectra up to $\ell \simeq 10^3$ are approximated very well by power laws with slope coefficients $\alpha_E \simeq \alpha_B \simeq 1.4$, a result very close to that of Prunet et al. (1998). The intensity spectrum is also found to have a moderate slope, close to that of polarization spectra, unless we use alternative maps (available at the Parkes WEB site⁷) where Galactic-plane sources have been removed; therefore this result should not be extrapolated to the whole sky. In the last section of this paper we provide reasons, suggesting that the slopes of polarization spectra are likely to

⁷ http://www.atnf.csiro.au/database/astro_data/2.4Gh_Southern

apply to the whole sky. We show that if this assumption is correct, synchrotron emission cannot be a problem for CMB polarization measurements in the cosmological window. Otherwise, a value $\simeq 1.4$ can be used as a *lower limit* to α_E and α_B ; then the slope differences with respect to the CMB polarization spectra would still be larger, and the CMB polarized signal would prevail even more strongly in the cosmological window.

2 Angular spectra in the Parkes survey

Figure 1 shows the sky coverage of the Parkes 2.417 GHz survey and other available surveys as well. The Parkes survey covers a strip, 127° long and at least 10° wide, with a FWHM resolution of $10'.4$. Maps are available at the Parkes WEB site for the total intensity I both before and after subtraction of structures with size $\leq 2^\circ$, and for the Stokes parameters Q and U with no source subtraction.

Because of the limited sky coverage, spherical-harmonic spectra are suitably obtained from a standard Fourier analysis according to the technique developed by Seljak (1997) for the CMB polarization and applied by Prunet et al. (1998) to the polarized dust foreground. After the Fourier components of Stokes parameters $I(\mathbf{l})$, $Q(\mathbf{l})$ and $U(\mathbf{l})$ are computed on a map covering a solid angle Ω , the estimators for the power spectra of intensity $C_{I\ell}$ and total polarization $C_{P\ell}$ can be readily computed by means of the equations

$$C_{I\ell} = \left\{ \frac{\Omega}{N_\ell} \sum_{\mathbf{l}} [I(\mathbf{l})I^*(\mathbf{l})] - w_I^{-1} \right\} b^{-2}(\ell), \quad (1)$$

$$C_{P\ell} = \left\{ \frac{\Omega}{N_\ell} \sum_{\mathbf{l}} [Q(\mathbf{l})Q^*(\mathbf{l}) + U(\mathbf{l})U^*(\mathbf{l})] - 2w_P^{-1} \right\} b^{-2}(\ell), \quad (2)$$

where the sums are performed over the N_ℓ modes with wavevector magnitude around ℓ , $b(\ell)$ is the window function and $w_{I,P}^{-1} = \Omega\sigma_{I,P}^2/N_{\text{pixel}}$ is the pixel-independent measure of noise with $\sigma_{I,P}$ the pixel noise. The electric and magnetic parity of polarization can also be separately computed by means of

$$C_{E\ell} = \left\{ \frac{\Omega}{N_\ell} \sum_{\mathbf{l}} |Q(\mathbf{l}) \cos(2\phi_{\mathbf{l}}) + U(\mathbf{l}) \sin(2\phi_{\mathbf{l}})|^2 - w_P^{-1} \right\} b^{-2}(\ell), \quad (3)$$

$$C_{B\ell} = \left\{ \frac{\Omega}{N_\ell} \sum_{\mathbf{l}} |-Q(\mathbf{l}) \sin(2\phi_{\mathbf{l}}) + U(\mathbf{l}) \cos(2\phi_{\mathbf{l}})|^2 - w_P^{-1} \right\} b^{-2}(\ell), \quad (4)$$

with $\phi_{\mathbf{l}}$ the direction angle of \mathbf{l} .

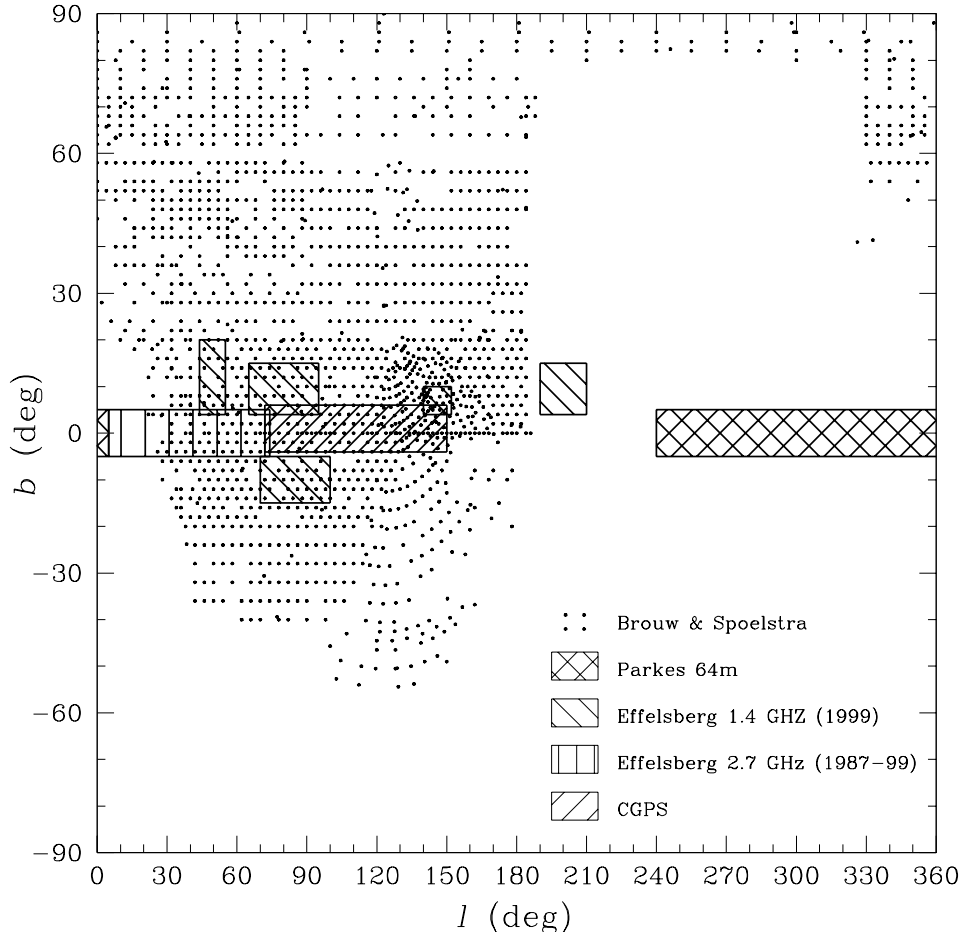


Fig. 1. Sky coverages of synchrotron polarization surveys. We report the regions observed at 0.408-1.411 GHz by Brouw & Spoelstra (1976); in the 2.417-GHz Parkes survey (Duncan et al., 1995, 1997); at Effelsberg, 2.695 GHz (Junkes et al. 1987; Duncan et al., 1999) and 1.4 GHz (Uyaniker et al. 1999); and in the Canadian Galactic Plane survey (CGPS, 0.408 and 1.420 GHz) (English et al., 1998).

For the Parkes survey the window function can be approximated by a Gaussian, $b(\ell) = \exp[-\ell(\ell + 1)\sigma_b^2/2]$ with $\sigma_b = 4'.4$. The polarization noise is not constant, being 11 mJy beam area⁻¹ for most of the sky coverage but as low as 6 mJy beam area⁻¹ in some regions. We chose to extract from the survey constant-noise square patches of $10^\circ \times 10^\circ$ (i.e., 150×150 pixels). We thereby obtained 12 independent submaps (the first one being centered at $l = 360^\circ$ and moving toward decreasing Galactic longitudes), and on each of them we performed the Fourier analysis and derived a set of four spectra $C_{X\ell}$ (with $X = I, P, E$ and B) by means of Eqs. (1)-(4) (the P spectrum was in fact redundant, but we computed it for all of the submaps for checks of consistency). A potential problem with the Fourier analysis, when it is applied to small maps, arises from border effects, which may give spurious contributions to the spectra. A solution to this problem is considered by Hobson & Magueijo

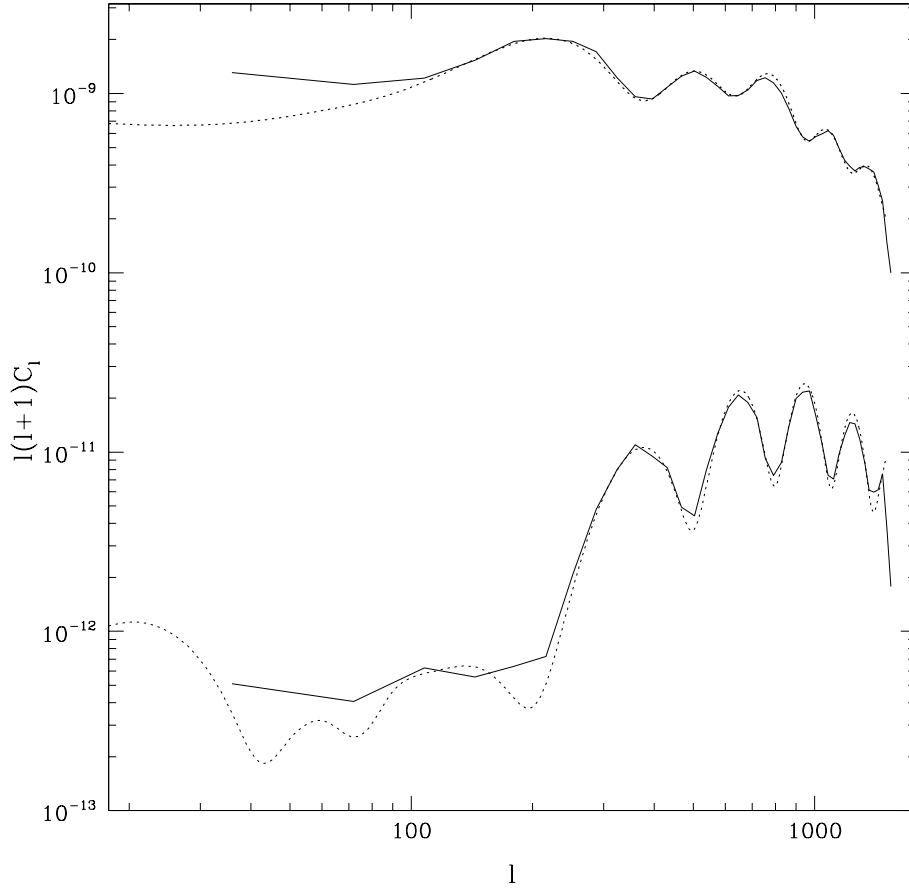
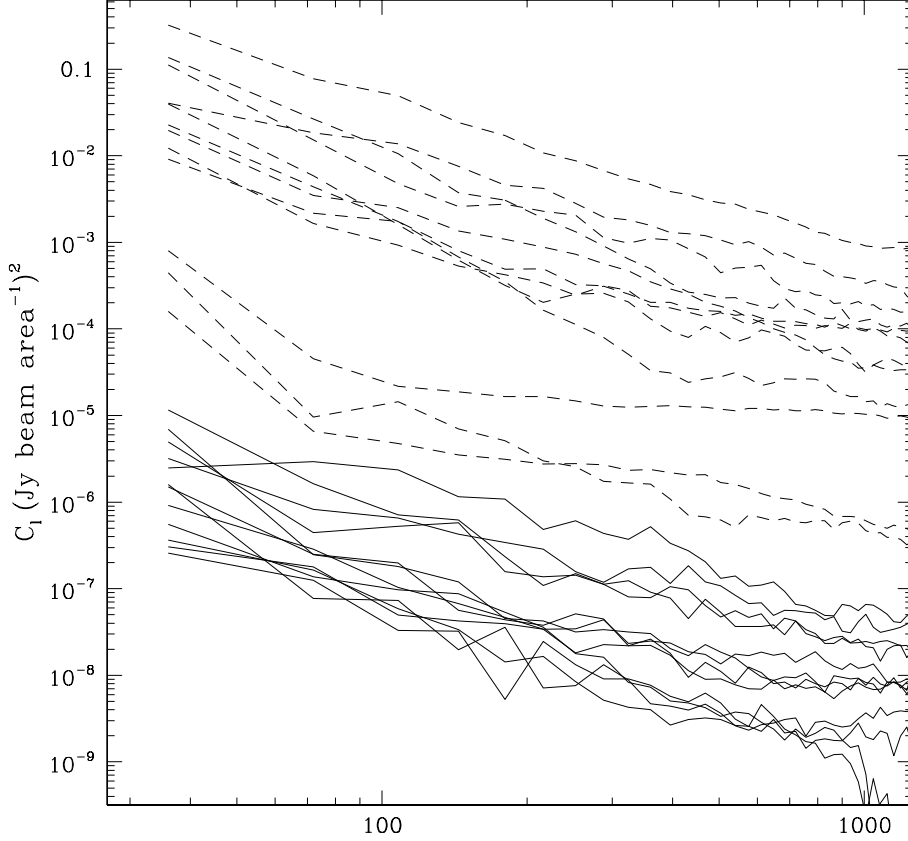


Fig. 2. The input and output CMB spectra (dotted and full line, respectively) for a test of Fourier analysis in the Parkes survey window. The input spectrum is computed for a standard CDM model with a secondary-ionization optical depth $\tau_{ion} = 0.18$.

(1996), who suggest to modulate the signal by some function vanishing at the borders (apodization). We carried out our analysis both with appropriate cosine functions and with no modulation. The differences turned out to be small in the range $\ell \lesssim 1000$, except for the intensity maps with source subtraction. In Figures 3-5 we explicitly report the results obtained with the cosine modulation up to $\ell = 1100$, which is close to the resolution limit of the survey. In order to test the reliability of the computed spectra, we also built up simulated maps for CMB, using angular spectra computed by means of CMBFAST (Seljak & Zaldarriaga, 1996) and HEALPix package⁸, and performed the Fourier analysis on them within the Parkes survey window. The results shown in Figure 2 prove that the method is quite reliable: The output spectrum differs from the input one only for some smoothing of the sharpest features, which is particularly evident for low values of ℓ . Smoother spectra – such as those expected for synchrotron – are less affected by the procedure. The results for all of the 12 submaps also are mutually consistent in the CMB

⁸ <http://www.tac.dk/healpix>



1

Fig. 3. The angular power spectra $C_{I\ell}$ and $C_{E\ell}$ (dashed and full lines, respectively) for the 12 submaps of the Parkes survey.

case.

The spectra obtained from synchrotron submaps, however, show large variations in the normalization; this fact is certainly not unexpected, due to the phase coherence of Galactic structure. Figure 3 shows the results for $C_{I\ell}$ (with no source subtraction) and $C_{E\ell}$ from the individual submaps; the results for magnetic parity polarization are similar to those for electric parity (the intensity spectra after source removal, however, are much steeper than those reported in the Figure, as we will discuss below).

The normalization variations for intensity and polarization cover different ranges (spanning more than 3 and about 2 orders of magnitude, respectively), and they are not strictly correlated since the polarization degree is far from being constant. The slopes of the curves up to $\ell \approx 10^3$, however, are much more mutually consistent than normalization. Visual inspection of Fig. 3 shows a couple of low-emission regions (submaps 9 and 12, placed at $l < 280^\circ$) with particularly flat intensity curves at $\ell \gtrsim 10^2$, but this feature does not appear in polarized emission. Clearly most of the curves are reasonably approximated by power laws, but when we fit the data with functions $C_{X\ell} = A_X \ell^{-\alpha_X}$, the

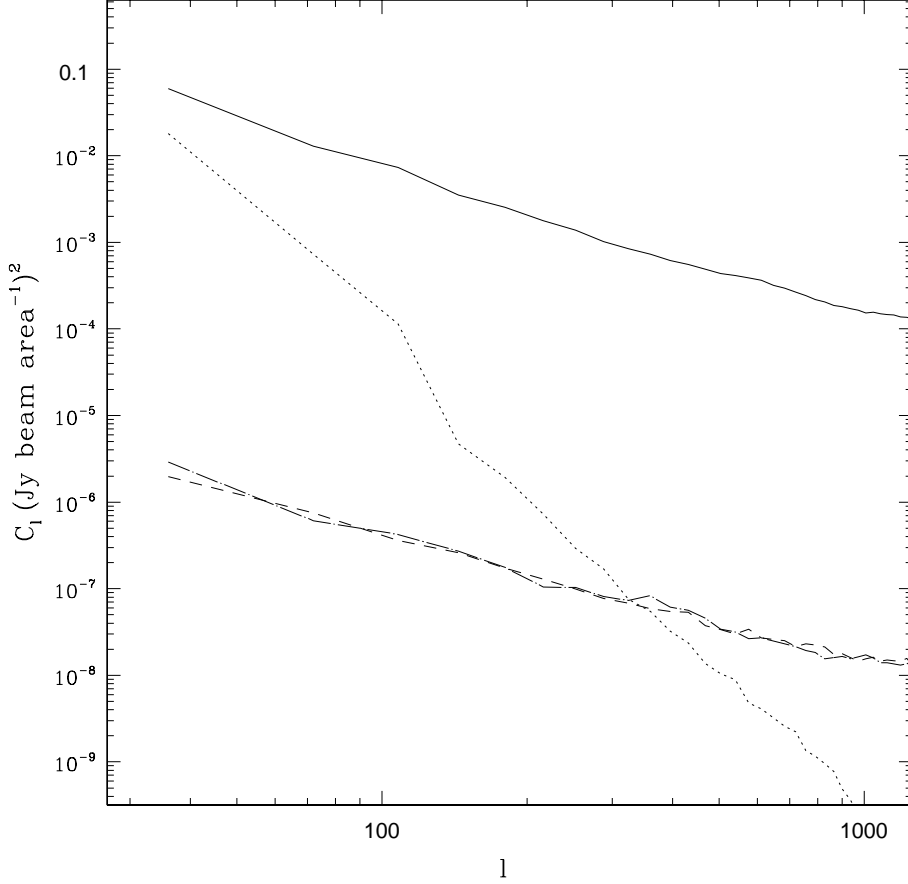


Fig. 4. The mean power spectra in the Parkes survey. The curves give the intensity $C_{I\ell}$ with and without source subtraction (full and dotted lines, respectively) and the polarization $C_{E\ell}$ and $C_{B\ell}$ (dash-dotted and dashed).

logarithmic slopes vary with both the chosen submap and the range of ℓ . In Table 1 we report angular-spectrum best-fit slopes for all of the submaps with no source subtraction. Columns 2 to 4 (primed quantities) refer to the range $\ell \leq 500$, and the remaining (unprimed quantities) to $\ell \leq 800$. Only for two submaps and for $\ell \leq 500$ the intensity spectra are steeper than $\alpha_I = 2$; more often they are only moderately steeper than polarization spectra, or even hardly distinguishable from them (as far as slopes are concerned).

We then have to combine the results from the 12 submaps in some way. A simple method is to compute weighted averages of the best-fit parameters; this implies weighting with statistical errors, with no regard to the strength of the emission in the submaps. Table 2 gives the mean parameters (including the normalization factors, denoted by A_X and A'_X) obtained in this way, as well as the statistical errors; they are collected in the Table rows referring to averaging “method 1”. According to such results, the slope of the intensity spectrum slightly decreases for increasing ℓ and can be hardly distinguished

Table 1

Best-fit slopes of angular power spectra in the Parkes survey submaps with no source subtraction

Submap	α'_I	α'_E	α'_B	α_I	α_E	α_B
1	1.79	1.05	1.24	1.65	1.28	1.33
2	1.50	1.28	1.25	1.64	0.85	1.12
3	2.54	1.29	1.45	2.00	1.31	1.52
4	1.98	1.74	2.06	1.46	1.57	1.74
5	2.87	1.56	1.47	1.76	1.49	1.40
6	1.65	1.16	1.18	1.89	1.11	0.96
7	1.56	1.39	1.78	1.22	1.56	1.88
8	1.56	2.26	1.98	1.43	2.04	1.90
9	0.74	1.78	2.02	0.44	1.56	1.78
10	1.23	1.28	1.23	1.02	1.79	1.25
11	1.97	1.83	1.61	1.48	1.48	1.32
12	0.76	2.09	1.68	0.96	1.58	1.45

Table 2

Best parameters for angular power spectra

X	Averaging method	A'_X Jy (beam area) ⁻¹	α'_X	A_X Jy (beam area) ⁻¹	α_X
I	1	241 ± 109	1.71 ± 0.18	17 ± 9	1.37 ± 0.13
I	2	28^{+27}_{-13}	1.79 ± 0.13	9.6^{+11}_{-5}	1.6 ± 0.13
I	2*	$(7.5^{+25}_{-5.3}) \cdot 10^{+5}$	5.2 ± 0.3	$(2.5^{+2.3}_{-1.6}) \cdot 10^{+5}$	5.0 ± 0.2
I	3	12^{+22}_{-9}	1.6 ± 0.2	$3.2^{+3.5}_{-1.8}$	1.36 ± 0.13
E	1	$(8.5 \pm 3.8) \cdot 10^{-4}$	1.57 ± 0.11	$(11.5 \pm 8.7) \cdot 10^{-4}$	1.44 ± 0.09
E	2	$(2.1^{+4.7}_{-1.6}) \cdot 10^{-4}$	1.37 ± 0.22	$(5.0^{+4.4}_{-2.5}) \cdot 10^{-4}$	1.53 ± 0.11
E	3	$(1.3^{+2.2}_{-0.9}) \cdot 10^{-4}$	1.31 ± 0.18	$(2.7 \pm 1.2) \cdot 10^{-4}$	1.45 ± 0.1
B	1	$(16 \pm 12) \cdot 10^{-4}$	1.58 ± 0.10	$(4.4 \pm 1.8) \cdot 10^{-4}$	1.46 ± 0.09
B	2	$(4.5^{+8}_{-3}) \cdot 10^{-4}$	$1.52^{+0.16}_{-0.20}$	$(2.8^{+3.1}_{-0.8}) \cdot 10^{-4}$	$1.43^{+0.13}_{-0.06}$
B	3	$(8.2^{+14}_{-5.6}) \cdot 10^{-4}$	1.35 ± 0.20	$(6.8^{+6.7}_{-3.9}) \cdot 10^{-4}$	1.32 ± 0.13

*After source subtraction

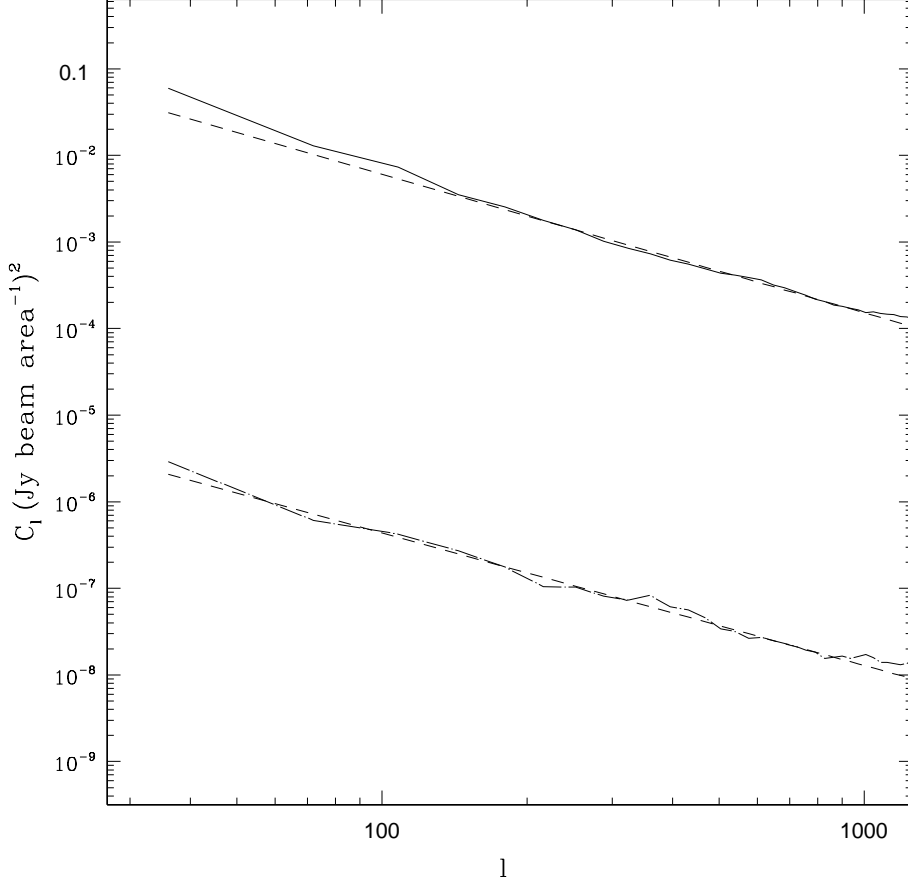


Fig. 5. The intensity and electric parity spectra compared to the fitting functions described in the text. The best-fit parameters refer to the range $36 \leq \ell \leq 800$ and to averaging “method 2”.

from that of polarization spectra at large ℓ :

$$\alpha_I \simeq \alpha_E \simeq \alpha_B \simeq 1.4 \div 1.5, \quad (\ell = 36 \div 800, \text{ method 1}). \quad (5)$$

Similar results are found with the simpler treatment with no signal cosine modulation; the differences with respect to the results in the Table are $\Delta\alpha_X \simeq \pm 0.1$.

It can be argued that because of the averaging method, the slopes given by Eq. (5) may be not representative of the full Parkes survey, since low-emission and high-emission subwindows are considered on equal footing. An alternative approach is averaging the spectra of the 12 subwindows: Figure 4 reports the mean spectra, and includes magnetic parity and the intensity spectrum after source subtraction. We thereby performed best fits as above also on such mean spectra. This procedure, referred to as averaging “method 2” in Table 2, clearly gives stronger weights to high-emission submaps. The results are quite different for the normalization factors (and especially for intensity), but no large variation is found for the slope factors. The slope of the intensity

spectrum however is slightly increased now, due to the scarce weight given to the nearly flat spectra of a couple of low-intensity submaps, the larger value being found in the smaller range $\ell = 36 \div 500$; no clear change however is found for polarization:

$$\alpha'_I \simeq 1.8, \quad \alpha'_E \simeq \alpha'_B \simeq 1.4 \div 1.5, \quad (\ell = 36 \div 500, \text{ method 2}). \quad (6)$$

As shown by Fig. 5, the fitting functions with the parameters found in the larger range ($\ell \leq 800$) describe very well the polarization spectra, whereas a modest discrepancy appears for the intensity spectrum at $\ell \leq 100$.

We also tried with a further procedure, renormalizing the spectra of the 12 submaps to a same mean intensity value and then constructing mean curves. The parameters of such mean curves are referred to as averaging “method 3” in the Table, and show slightly smaller slopes. For the range $\ell = 36 \div 800$

$$\alpha_I \simeq \alpha_E \simeq \alpha_B \simeq 1.4, \quad (\ell = 36 \div 800, \text{ method 3}). \quad (7)$$

A quite different result is found for the intensity maps with source subtraction. The slope is now much higher, $\alpha_I \simeq 5$. At large ℓ the signal is very small, and it would be overcome by border effects in the absence of apodization even for $\ell < 10^3$.

3 Discussion

The most attractive conclusion we can draw from the present work regards the angular spectrum slope of the polarized synchrotron emission up to $\ell \approx 10^3$. Since this slope substantially differs from that of polarized CMB, provided it can be extrapolated to the cosmological window the separation of cosmological and Galactic signals becomes easier. In particular, at a given frequency CMB polarization is expected to prevail better at smaller scales; this result is derived from Galactic-plane maps with no source subtraction. It is interesting to observe that essentially the same slope, $\alpha_E \simeq \alpha_B \simeq 1.4$, was found by Prunet et al. (1998) for polarized dust emission. We may speculate that this coincidence may be due to the similarity of polarizing/depolarizing mechanisms inscribed in the Galactic structure.

On the other hand, our results on the total intensity spectrum might look somewhat intriguing at first sight. The original Parkes maps with no source subtraction support only a moderate slope, close to that of polarization spectra. This contrasts sharply with the results of Tegmark & Efstathiou (1996), Bouchet et al. (1996) and Bouchet & Gispert (1999); the discrepancy is much

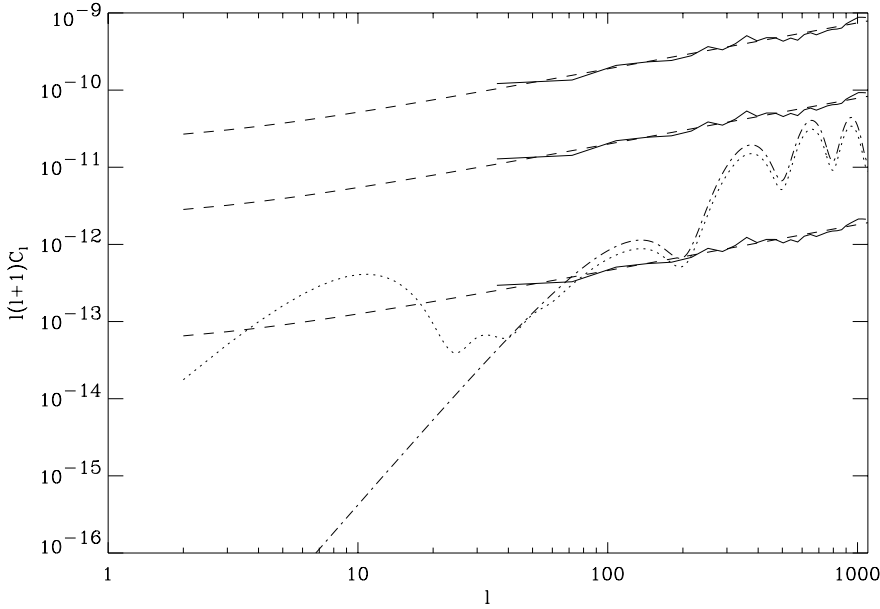


Fig. 6. The angular spectra of polarized synchrotron extrapolated to 22, 32, and 60 GHz (full line, from top to down) with the linear fits (dashed line), compared to the CMB E-spectrum computed for a standard CDM model (dot-dashed line) and a CDM with a secondary ionization optical depth $\tau_{ion} = 0.2$ (dotted line).

smaller with the analysis of Lasenby (1997) on the Tenerife patch. Removal of sources up to 2° wide, however, gives a much larger slope, beyond the more familiar result $\alpha_I \approx 3$. This fact can be readily interpreted, observing that in the Parkes survey the intensity angular spectrum at large ℓ is dominated by Galactic-plane sources. An obvious consequence is that no real contradiction exists with previous work, since such results as $\alpha_I \simeq 1.4 \div 1.8$ cannot be extrapolated outside the Galactic plane.

We then should ask, which values of α_X would be appropriate for the whole sky. Clearly the subtraction of 2° sources as described at the Parkes WEB site is a quite radical procedure, cutting out high-order harmonics very efficiently. It is then easy to infer that the full-sky α_I must lie somewhere between 1.4 and 5; however the existing support for the value $\alpha_I \approx 3$ is not very strong, in view of the results of Lasenby (1997), supporting $\alpha_I \approx 2$. On the other hand, we believe that our results on the polarization slope can be extrapolated out of the Galactic plane with some confidence. The inspection of Fig. 3 shows that for polarization no systematic differences of slope exist between high and low emission submaps. As already remarked, the overall normalization (rms signal) has much weaker variations than for intensity spectra. Thus the role of Galactic-plane sources is less important. Also, the agreement with Prunet et al. (1998) is impressive.

Assuming that the polarization angular spectra are correct for the full sky, we

can try to extrapolate them to frequencies higher than 2.4 GHz and compare them to CMB spectra. Figure 6 shows such extrapolations to 22, 32 and 60 GHz, where the average Parkes survey normalization and a synchrotron spectral index of 3 are assumed. Obviously this procedure is expected to overrate the synchrotron full-sky spectra. The comparison of synchrotron and CMB angular spectra shows that for $\ell > 10^2$ the latter prevail at 60 GHz in spite of the above Galactic-plane normalization.

Finally, we may ask how this conclusion should be changed if the polarization slopes of Table 2 cannot apply to a full-sky survey. According to the reasoning expounded for intensity spectra, we can state that values $\simeq 1.4$ can *at least* be used as lower limits to α_E and α_B . Then the slope differences with respect to the CMB polarization spectra would still increase in comparison with the scenario described by Fig. 6, and the CMB signal would prevail even more strongly in the cosmological window.

Acknowledgments

We thank S. Bonometto and all the people of the SPORt collaboration team for help and encouragement. M. Tucci wishes to thank D. Scott for stimulating discussions. We acknowledge use of the CMBFAST code and the HEALPix package. This work is supported by the Italian Space Agency (ASI).

References

- [1] Barreiro, R.B., 1999, preprint astro-ph/9907094.
- [2] Bouchet, F.R., & Gispert, R., 1999, *NewA*, 4, 443.
- [3] Bouchet, F.R., Gispert, R., & Puget, J.L., 1996, in: *Unveiling the Cosmic Infrared Background*, Dwek, E. (Ed.), AIP (Baltimore).
- [4] Brouw, W.N., & Spoelstra, T.A., 1976, *A&AS*, 26, 129.
- [5] Cortiglioni, S., et al., 1999, in: *3 K Cosmology*, Maiani, L., Melchiorri, F. & Vittorio, N. (Eds.), AIP Conference Proc. 476, 186; and SPORt home page: <http://tonno.tesre.bo.cnr.it/~sport/>.
- [6] De Bernardis, P., et al., 2000, *Nature*, 404, 955.
- [7] De Zotti, G., et al., 1999, in: *3 K Cosmology*, Maiani, L., Melchiorri, F. & Vittorio, N. (Eds.), AIP Conference Proc. 476, 204; and PLANCK home page: <http://astro.estec.esa.nl/SA-general/Projects/Planck>.
- [8] Draine, B.T., & Lazarian, A., 1998, *ApJ*, 494, L19.

- [9] Duncan, A.R., Haynes, R.F., Jones, K.L., & Stewart, R.T., 1997, MNRAS, 291, 279.
- [10] Duncan, A.R., Stewart, R.T., Haynes, R.F., & Jones, K.L., 1995, MNRAS, 277, 36.
- [11] Duncan, A.R., Reich, P., Reich, W. & Fürst, E., 1999, A&A, 350, 447
- [12] English, J., et al., 1998, Pub. Astron. Soc. Australia, 15, 56; and CGPS home page: <http://www.ras.ucalgary.ca/CGPS>.
- [13] Gautier, T.N., Boulanger, F., Perault, M., & Puget, J.L., 1992, AJ, 103, 1313.
- [14] Hanany, S., et al., 2000, preprint astro-ph/0005123.
- [15] Haslam, C.G.T., et al., 1981, A&A, 100, 209.
- [16] Hedman, M., 1999, available at PIQUE home page: <http://physics.Princeton.edu/~paladino/pique.htmlx>.
- [17] Hobson, M.P., & Magueijo, J., 1996, MNRAS, 283, 1133.
- [18] Junkes, N., Fürst, E., Reich, W., 1987, A&AS, 69, 451.
- [19] Keating, B., Timbie, P., Polnarev, A.G., & Steinberger, 1998, ApJ, 495, 580.
- [20] Kogut, A., et al., 1996, ApJ, 460, 1.
- [21] Lasenby, A.N., 1997, in: Microwave Background Anisotropies, Proc. XVI Moriond Astrophysics Meeting, Bouchet, F.R., Gispert, R., Guiderdoni, B., & Tran Van, J. (Eds.), Editions Frontieres (Paris, France), p. 453.
- [22] Pisano, G., 1999, NewAR, 43, 329.
- [23] Prunet, S., Sethi, S.K., & Bouchet, F.R., 2000, MNRAS, 314, 348.
- [24] Prunet, S., & Lazarian, A., 1999, in: Microwave Foregrounds, de Oliveira-Costa, A., & Tegmark, M. (Eds.), ASP (San Francisco).
- [25] Prunet, S., Sethi, S.K., Bouchet, F.R., & Miville-Deschenes, M.-A., 1998, A&A, 339, 187.
- [26] Reich, P., & Reich, W., 1986, A&AS, 63, 205.
- [27] Schlegel, D.J., Finkbeiner, D.P., & Davis, M., 1998, ApJ, 500, 525.
- [28] Seljak, U., 1997, ApJ, 482, 6.
- [29] Seljak, U., & Zaldarriaga, M., 1996, ApJ, 469, 437.
- [30] Sethi, S.K., Prunet, S., & Bouchet, F.R., 1998, in : Fundamental Parameters in Cosmology, XXXIII Rencontres de Moriond, Tran Than Van, J., & Giraud-Heraud, Y. (Eds.), Editions Frontieres (Paris, France).
- [31] Sironi, G., et al., 1997, NewA, 3, 1.

- [32] Spoelstra, T.A.T., 1984, *A&A*, 135, 238.
- [33] Tegmark, M., Eisenstein, D.J., Hu, W., & de Oliveira-Costa, A., 2000, *ApJ*, 530, 133.
- [34] Tegmark, M., & Efstathiou, G., 1996, *MNRAS*, 281, 1297.
- [35] Uyaniker, B., et al., 1999, *A&AS*, 138, 31.
- [36] Veeraravaghan, S., & Davies, R.D., 1997, in: *Proc. Particle Physics and the Early Universe Conference*, University of Cambridge, 7-11 April 1997, available at PPEUC home page: http://www.mrao.cam.ac.uk/ppeuc/proceedings/cmb_prog.html.
- [37] Wieringa, M.H., de Bruyn, A.G., Jansen, D., Brouw, W.N., & Katgert, P., 1993, *A&A*, 268, 215.
- [38] Wright, E.L., 1998, *ApJ*, 496, 1.
- [39] Wright, E.L., 1999, *NewAR*, 43, 257; and MAP home page: <http://map.gsfc.nasa.gov>.